Random Crystal and Magnetic Field Effects on Hysteresis Loops and Phase Transition of Blume–Capel Model in Cluster Variation Method

R.A.A. Yessoufou[a,b], A. Kpadonou[a,c], G. Seto[a] and E. Albayrak[d,*]

[a] *Institute of Mathematic and Physical Sciences (IMSP), Dangbo, Benin*
[b] *University of Abomey-Calavi, Department of Physics, Calavi, Republic of Benin*
[c] *UNSTIM, ENS-Natitingou, Laboratory of Physics and Applications (LPA), Abomey, Benin*
[d] *Erciyes University, Department of Physics, 38039, Kayseri, Turkey*

Received: 16.03.2022 & Accepted: 26.04.2022

Doi: 10.12693/APhysPolA.141.634 *e-mail: albayrak@erciyes.edu.tr

The effects of bimodal random crystal field and trimodal magnetic field distributions on the order parameters, i.e., magnetization and quadrupole moments, susceptibility and hysteresis properties of the spin-1 Blume–Capel model are investigated. The lowest approximation of the cluster variation method was used. For the distributions of crystal field and magnetic field, two nodes and three nodes distributions were chosen, respectively, with the probabilities q and p. Exploiting the variation of the order parameters and susceptibility as functions of temperature and crystal field, it was found that they exhibit either continuous or discontinuous phase transitions, i.e., first- or second-order, respectively. The model also presents the re-entrant behaviour for some values of our system parameters. Under the constraint of magnetic field and specific values of the system parameters, two, four and six hysteresis loops have been observed.

topics: Blume–Capel model, bimodal crystal field, trimodal magnetic field, reentrant behaviour

1. Introduction

To overcome the difficulties presented by magnetic many-body systems with many interactions, approximate methods are required which at least make it possible to reveal the rich magnetic properties of the system, since exact solution methods either do not exist or are not useful. Weiss [1] therefore proposed a mean-field approach where the many-body problem is reduced to the one-body problem and interactions affecting the body are replaced by the effective field. In this approach, the spin correlations are neglected and the transition temperature is overestimated. In order to improve these ideas, Hans Bethe [2] proposed an approach which takes into account the central-spin forming the cluster with its near-neighbor spins — via this way the spin correlations are included. Later, Kikuchi [3] developed the cluster variation method (CVM) which allows one to construct approximate solutions for free energy in the thermodynamic limit from solutions for finite clusters, and which provides better results compared to the ordinary mean-field theory [4]. Among the physical models that can describe these systems is the Blume–Capel (BC) model [5, 6], which was initially used to study the critical behaviour of He^3–He^4 mixture in random media [7]. Recent advances in phase transitions and critical phenomena are reviewed in [8], in addition to the importance of the BC model. Taking into account random crystal field or magnetic field in this model made it possible to describe disordered systems, such as single-spin and mixed-spin systems [9–11], the spin-glass models [12, 13], the ternary alloys [14–17] etc., all of which exhibit rich properties.

The random transverse crystal field effects on the spin-1 BC model were considered in the mean-field (MF) approximation [18]. This approach was also used to study the effects of transverse and longitudinal external magnetic fields added to the random longitudinal crystal field for the spin-1 BC model [19]. Based on the exact recursion relations, the $\pm J$ spin-1 BC model was investigated on the Bethe lattice, and the glass phase and two special points were observed [20, 21]. Using high-precision Monte Carlo simulations and finite-size scaling, the effect of quenched disorder in exchange couplings on the BC model [22] was examined on a square lattice with the addition of a parallel version of the Wang–Landau algorithm [23]. Using the framework of the effective field theory (EFT) based on the probability

distribution technique, the hysteresis behaviour of the spin-1 BC ferromagnetic (FM) and ferrimagnetic (FI) nano islands were investigated and multiple hysteresis loops were found [24]. The spin-1 BC model was also studied by using EFT [25] or EFT with correlation [26], a new approach of MFT [27], MFT based on Bogoliubov inequality [28], pair approximation (PA) [29, 30], Monte Carlo (MC) simulations [31] and CVM [32, 33].

It should also be noted that the effects of a random magnetic field were also studied in some other works. Numerical simulations and finite-size scaling techniques were applied to investigate the properties of the dynamic phase transition in the BC model subjected to a periodically oscillating field [34]. The bimodal random field with equal probability was implemented on the spin-1 BC model and was examined in the MFT and exact recursion relations. As a result, isolated ordered critical end-points, critical lines with two tricritical points and other types of critical points [35–37] were observed. Recently, investigation of the same model using the CVM has shown that, in addition to tricritical behaviours, single and double hysteresis loops were observed [38]. The trimodal field distribution was first used in the case of the random-field Ising model and several important results have been obtained for the critical properties of the $d = 3$ random-field Ising model with an equal weight trimodal distribution at zero temperature [39]. In addition, the effects of the trimodal random field were also studied that induce not only the critical points, reentrant and double reentrant behaviours, but also the multiple hysteresis loops [40, 41].

In all these works [18–41], however, no investigation was done on the spin-1 BC model both for a random crystal and magnetic fields. Thus, the aim of this study is to investigate the variations of the order parameters, susceptibility and hysteresis properties in this spin system under the simultaneous effects of a trimodal random magnetic and a bimodal random crystal fields. For this, we use the lowest approximation of the CVM (LACVM). In fact, we were motivated by the fact that the consideration of the effects of bimodal random crystal field and trimodal random magnetic field on the spin-$\frac{3}{2}$ BC model resulted in very interesting and attractive critical behaviours for some critical random parameters values [42].

This paper is structured as follows: in Sect. 2, we briefly describe the model and formulate it using the LACVM. In Sect. 3, we discuss the obtained numerical results. The last section takes into account the conclusions.

2. The model and formalism

The Hamiltonian of the BC model with only the nearest-neighbor (NN) bilinear interaction parameter $J > 0$ for a random crystal and the magnetic fields D_i and h_i, can be expressed as

$$H = -J \sum_{<i,j>} S_i S_j - \sum_i D_i (S_i)^2 - \sum_i h_i S_i, \tag{1}$$

where S_i is the spin-1 operator, which assumes the value $\pm 1, 0$ at the site i. The random distributions of the magnetic h_i and crystal field D_i are given as

$$P(h_i) = p\,\delta(h_i) + \frac{(1-p)}{2}\Big[\delta(h_i - h) + \delta(h_i + h)\Big] \tag{2}$$

and

$$P(D_i) = q\,\delta\big(D_i\big) + (1-q)\,\delta\big(D_i - D\big) \tag{3}$$

with three and two nodes. Importantly, $P(h_i)$ is distributed in such a way that a portion p of the spins is not subjected to any magnetic field, while the other two portions are under the influence of the magnetic field h and $-h$ along the same axis with the same probability $(1-p)/2$. Regarding $P(D_i)$, some spins are free from crystal field effects with probability q and the rest are under the action of crystal field D with probability $(1-q)$.

Before giving the formulation of the model presented here, let us give a bit of information about the CVM. It was first introduced by Kikuchi [3] in 1951 as an approximation of the equilibrium statistical mechanics of lattice (Ising-like) models, generalizing the Bethe–Peierls [43] and Kramers–Wannier [44, 45] approximations which can be found in several textbooks [46, 47]. In addition to reviving these methods, Kikuchi proposed a combinatorial derivation of what today we can call the cube (respectively triangle, tetrahedron) approximation of the CVM for the Ising model on a simple cubic (respectively triangular, face-centered cubic) lattice. After the first proposal, many reformulations and applications appeared, mainly to the computation of phase diagram of lattice models in statistical physics and material science, and these were reviewed in [48]. In most applications, the CVM does not yield exact results, and hence it is worth investigating its properties, as an approximation. The CVM is known to be exact in several cases due to the topology of the underlying graph or to the special form of the Hamiltonian. More details on the CVM can be found in the review given by [49].

In the CVM, each spin state is characterized by the average values denoted by X_1, X_2 and X_3, which represent a fraction of the spins with the value $+1$, 0 and -1, respectively. The normalization relation they obey is written as

$$\sum_i X_i = 1. \tag{4}$$

To study this model, one needs to define two long-range order parameters, i.e, the magnetization $M = \langle S_i \rangle$ and the quadrupole moment $Q = \langle S_i^2 \rangle$. Considering the internal variables previously defined, the expressions of order parameters are given by

$$M = X_1 - X_3, \quad Q = X_1 + X_3. \tag{5}$$

The expressions for the internal variables as functions of the order parameters are obtained from (5) and written as

$$X_1 = \frac{(M+Q)}{2}, \quad X_2 = (1-Q), \quad X_3 = -\frac{(M-Q)}{2}. \tag{6}$$

The LACVM [1, 50] is employed to determine the equilibrium properties, which gives similar results as the MF approximation. This method consists of three steps: (i) take a collection of weakly interacting systems, (ii) define the state variables and obtaine the weight factors in terms of the state variables and finally (iii) find the free energy expression and minimize it.

The weight factors are defined as a function of the internal variables as follows

$$W = \frac{N!}{\prod_{i=1}^{3}(X_i N)!}, \tag{7}$$

where N is the number of lattice points. The internal energy of the model can be calculated as a function of the order parameters using

$$\frac{E}{N} = -J\,M^2 - D_i\,Q - h_i\,M. \tag{8}$$

By inserting the internal variables (6) into (8), one obtains the internal energy per unit atom as

$$\frac{E}{N} = -J\,(X_1 - X_3)^2 - D_i\,(X_1 + X_3) - h_i\,(X_1 - X_3). \tag{9}$$

Using the definition of entropy $S = k_{\mathrm{B}} \log(W)$ and the Stirling approximation, the free energy $F = E - TS$ per lattice site can be expressed by

$$\begin{aligned}\Phi = -\frac{\beta F}{N} &= \beta J(X_1 - X_3)^2 + \beta D_i(X_1 + X_3) \\ &+ \beta h_i(X_1 - X_3) - \sum_{i=1}^{3} X_i \ln(X_i) \\ &+ \lambda\Big(1 - \sum_{i=1}^{3} X_i\Big),\end{aligned} \tag{10}$$

where λ is introduced to satisfy the normalization condition and k_{B} is the Boltzmann constant. By minimizing (10) with respect to X_i, i.e.,

$$\frac{\partial \Phi}{\partial X_i} = 0, \quad \text{with} \quad i = 1, 2, 3, \tag{11}$$

one can obtain the self-consistent equations for the magnetization and the quadrupolar moment, which are explicitly expressed as

$$M(D_i, h_i) = \frac{2\sinh\big(2\beta J\,M(D_i, h_i) + \beta h_i\big)}{\exp(-\beta D_i) + 2\cosh\Big(2\beta J\,M(D_i, h_i) + \beta h_i\Big)} \tag{12}$$

and

$$Q(D_i, h_i) = \frac{2\cosh\big(2\beta J\,M(D_i, h_i) + \beta h_i\big)}{\exp(-\beta D_i) + 2\cosh + 2\cosh\big(2\beta J M(D_i, h_i) + \beta h_i\big)}. \tag{13}$$

By integrating (11) and (12) over these distributions functions, one gets the integral form of the order parameters which are written as follows

$$M = \iint \mathrm{d}D_i\,\mathrm{d}h_i\,M(D_i, h_i)\,P(D_i)\,P(h_i) \tag{14}$$

and

$$Q = \iint \mathrm{d}D_i\,\mathrm{d}h_i\,Q(D_i, h_i)\,P(D_i)\,P(h_i). \tag{15}$$

The final forms of the order parameters are given as

$$\begin{aligned}M &= pq\,M(0,0) + p(1-q)\,M(D,0) \\ &+ \frac{(1-p)q\,\big[M(0,-h) + M(0,+h)\big]}{2} \\ &+ \frac{(1-p)(1-q)\big[M(D,-h) + M(D,+h)\big]}{2}\end{aligned} \tag{16}$$

and

$$\begin{aligned}Q &= pq\,Q(0,0) + p(1-q)\,Q(D,0) \\ &+ \frac{(1-p)\,q}{2}\big[Q(0,-h) + Q(0,+h)\big] \\ &\times \frac{(1-p)(1-q)\,\big[Q(D,-h) + Q(D,+h)\big]}{2}.\end{aligned} \tag{17}$$

The magnetic susceptibility of the system can be obtained with

$$\chi = \lim_{h \to 0} \frac{\partial M}{\partial h}. \tag{18}$$

By solving numerically (16) and (17) and using an iterative procedure, we then present the behaviour of the order parameters, susceptibility and hysteresis properties of our model. It should be mentioned that the iteration is stopped at each temperature step when the change of the order parameters become negligibly small, i.e., when they stabilize converging to their desired values.

3. Results and discussions

In this section, we first illustrate and discuss the variations of the order parameters and susceptibility by singling out the nature of the phase transition of the model, and then presenting its hysteresis properties.

3.1. Order-parameters and susceptibility variations

It should be noted that the model is the well-known BC model for $p = 1$ and $q = 0$. It reduces to the bimodal random magnetic BC model with equal probability for $p = 0$ and $q = 0$ and when the crystal field is turned off for $(p = 0, q = 1)$. Further, the model reduces to the spin-1 model with only NN interactions for $(p = 1, q = 1)$, and for all other values (p, q) our present model is recovered.

Thermal variations of magnetization and susceptibility are calculated when the magnetic field is turned off and on. In normal situations, the BC model does not give any phase transitions when $h \neq 0.0$. As seen from (2) for $P(h_i)$, one node

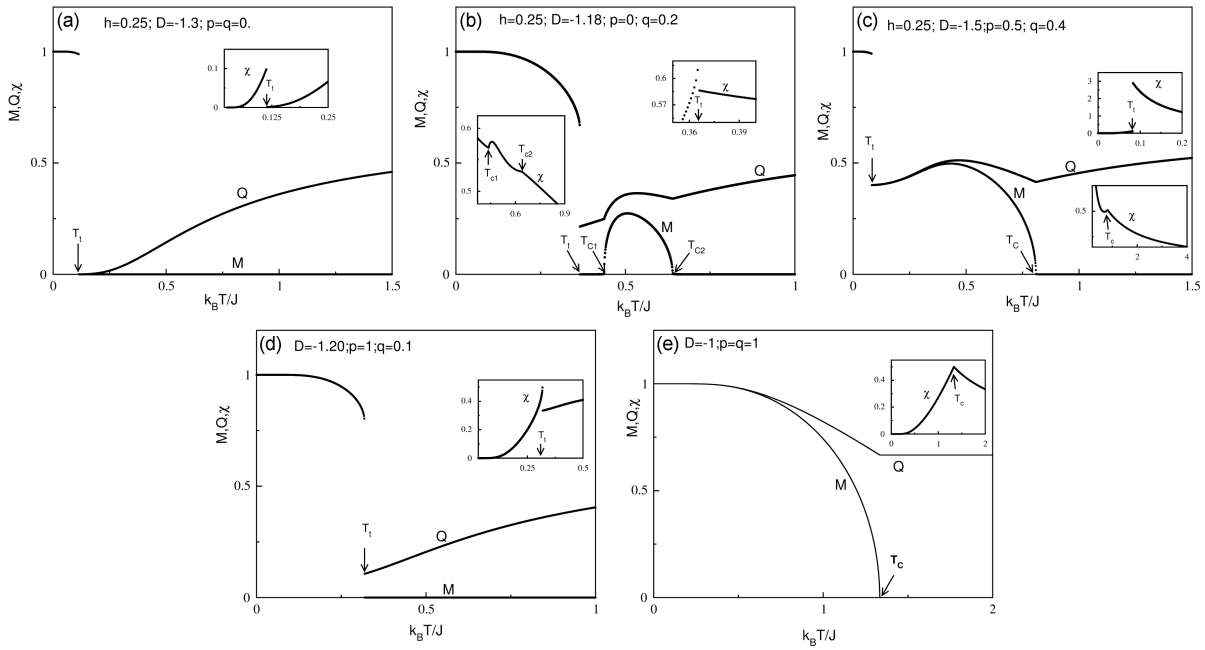

Fig. 1. Thermal behaviours of the order parameters and magnetic susceptibility for $h = 0.25$ and the values of (D, p, q) given as (a) $(-1.3, 0, 0)$, (b) $(-1.18, 0, 0.2)$ and (c) $(-1.5, 0.5, 0.4)$, and for $h = 0.0$ with (d) $(-1.20, 1, 0.1)$ and (e) $(-1, 1, 1)$. Temperatures T_t and T_c indicate the first- and second-order phase transition, respectively.

already gives $h = 0$ and the other two nodes turn on h with equal probability along the same axis in opposite directions. This equal probability is the reason for the appearance of the phase transitions. Figure 1a–c illustrate this when $h = 0.25$ with the existence of first- and second-order phase transition temperatures, denoted as T_t and T_c, respectively.

Figure 1a shows that the magnetization M and quadrupolar moment Q presenting discontinuous jumps at T_t indicate a first-order phase transition between ordered and disordered phases when $D = -1.3$ and $p = q = 0$. Afterwards, M always remains zero and Q increases from T_t to its limiting value of $\frac{2}{3}$ at higher temperatures. The thermal variation of χ shown in the inset exhibits that it first increases rapidly reaching a peak at T_t, then jumps to zero and then increases again.

In Fig. 1b, the model presents the temperature T_t first, and then the two temperatures T_c's, calculated for $D = -1.18$, $p = 0$ and $q = 0.2$. Indeed, M jumps from the FM to paramagnetic (PM) phase at T_t where it becomes zero and is still zero for some temperature range. It then reappears at T_{c1} enclosing the FM phase which then disappears at T_{c2} going into the PM phase. The quadrupolar moment Q also presents a jump at T_t and then starts increasing with increasing temperature, and on its way, it presents little kinks at T_{c1} and T_{c2}. The increase continues again towards the limit value of $\frac{2}{3}$. The insets of Fig. 1b show that the magnetic susceptibility χ increases rapidly until reaching a peak at T_t, then jumps and decreases to reach the critical point at T_{c_1} and then decreases to the second critical point at T_{c_2}, where little cusps are presented, and χ finally disappears. These observed behaviours indicate that the model changes from the FM to PM phase at T_t, then it passes from the PM phase to the FM phase again at T_{c_1} before re-entering again the PM phase one last time, at T_{c_2}. Thus, the existence of two temperatures T_c leads to the reentrant behaviour which is due to the competition between the entropy and the free energy of the system.

Figure 1c plotted for $D = -1.5$, $p = 0.5$ and $q = 0.4$ exhibits the temperature T_t first and T_c afterwards. In the case of M and Q, they start from their ground state value and do not change much as the temperature increases. Their jumps are presented at T_t and then at T_c, which is just before going into the PM phase. At low temperatures, χ is very close to zero becasue M changes very slowly. Then χ jumps to higher values, and as the temperature increases, it tends to zero, preceded by a little kink.

Figure 1d and e realized for $D = -1.2$, $p = 1$, $q = 0.1$ and $D = -1.0$ and $p = q = 1.0$ shows the well-known behaviours at T_t and T_c, respectively, when $h = 0.0$. Note that the increase in χ when the order parameters present only a transition at T_t, as in Fig. 1a and d, is interesting as the χ behaviour should rather gradually go to zero with increasing temperatures. The reason for the increase may be caused by the existence of the bimodal magnetic field with $p = 0$.

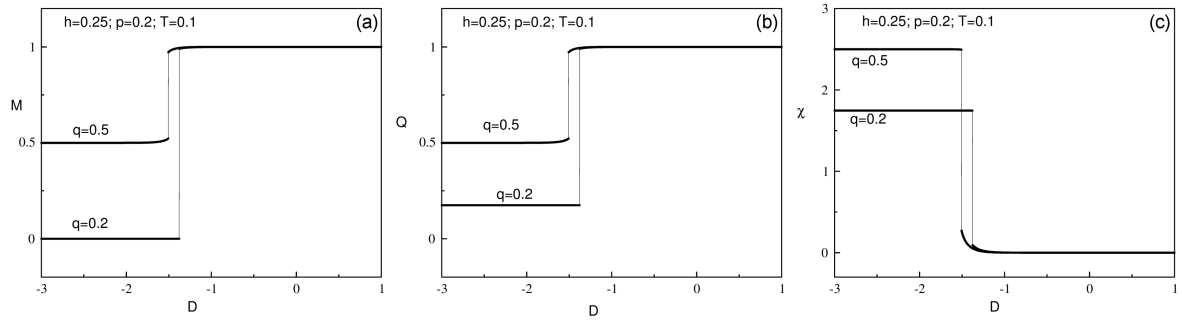

Fig. 2. Order-parameters and susceptibility versus the random crystal field D for the case with $p = 0.2$, $h = 0.25$ and the two different values of $q = 0.2$ and 0.5.

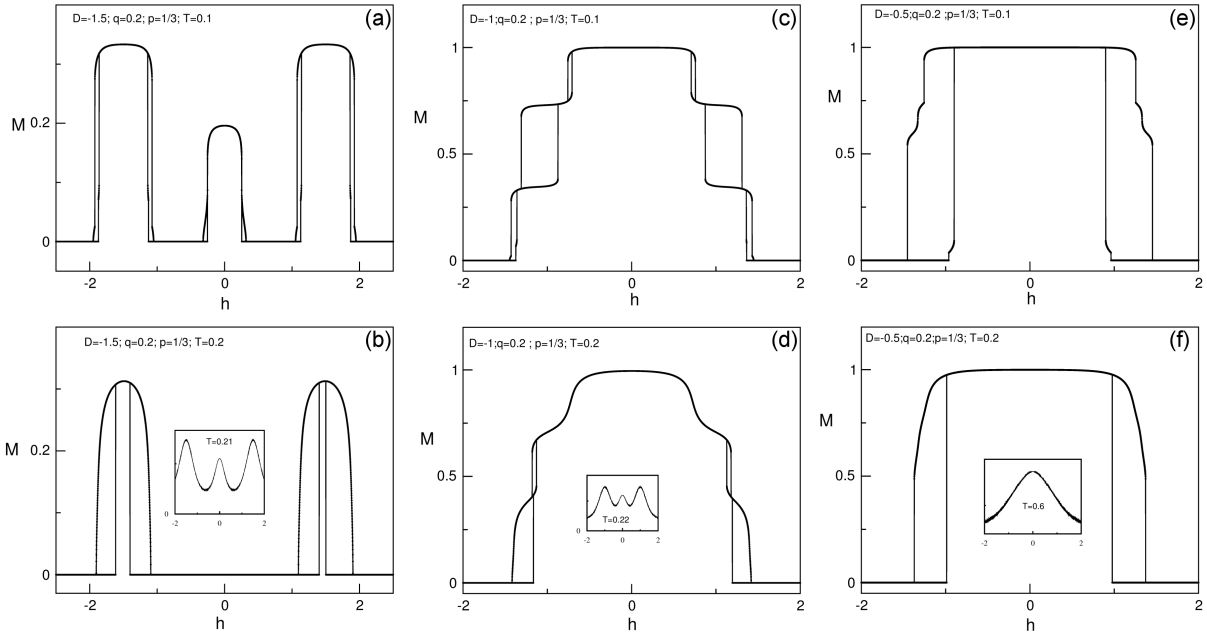

Fig. 3. Hysteresis behaviour of the system as a function of the applied field h at $T = 0.1$ or $T = 0.2$, $p = 1/3$, $q = 0.2$ when (a, b) $D = -1.5$, (c, d) $D = -1$ and, (e, f) $D = -0.5$.

In Fig. 2, we have presented the D variation of the order parameters and susceptibility at low temperatures for the values $T = 0.1$, $h = 0.25$, $p = 0.2$ when $q = 0.2$ and $q = 0.5$. The two plateaus shown correspond to the lower and higher D-values, and the jumps between them correspond to the first-order phase transitions. The jumps are seen first between the disordered and ordered phases for $q = 0.2$ and between the two ordered phases for $q = 0.5$. The magnetization value which characterizes each of these regions are $M = 0$, $M = \frac{1}{2}$ and $M = 1$. The value of $M = \frac{1}{2}$ corresponds to the case where the lattice is half–half covered by a couple of ground state values $(0, 1)$. It is also clear that at low negative values of D the order parameters are small, and for higher values they are higher. The reason for this is that the low negative values of D drive the system to the lowest value of spin-1 which is zero, otherwise ± 1 at higher D.

3.2. The hysteresis properties

We now explore the magnetic response of our system when the external magnetic field varies between two opposite values. Various forms of hysteresis loops have been obtained and constructed in Figs. 3–5 for low temperatures.

Figure 3 are plotted for various fixed values of D and T when $p = 1/3$ and $q = 0.2$. As can be observed, multiple hysteresis behaviours of 6 (a, c), 4 (b, d) and 2 (e, f) loops are obtained. It is noticed that for large negative values of D, the number of hysteresis loops increases and it decreases with increasing temperatures. Thus, the hysteresis loops disappear at $T = 0.21$, 0.22 and 0.6, respectively, when $D = -1.5$, -1 and -0.5.

Figure 4 obtained for $q = 0.5$ and maintaining other parameters as in Fig. 3, only show the existence of double hysteresis loops for $D = -1.5$, -1 and -0.5. Note that the rising temperature T or

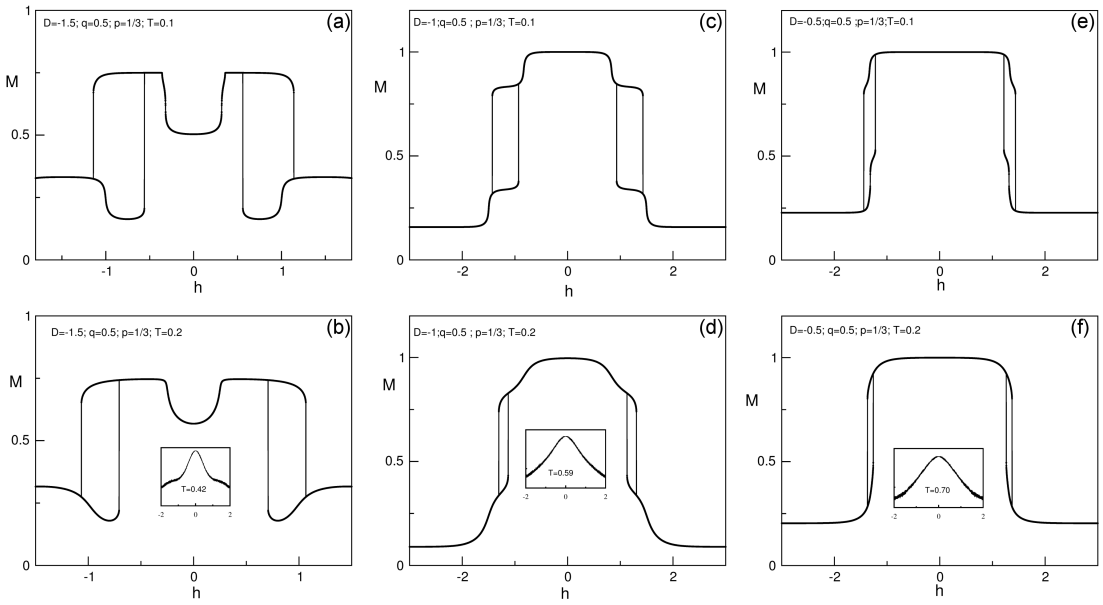

Fig. 4. Hysteresis behaviour of the system as a function of the applied field h at $T = 0.1$ or $T = 0.2$, $p = 1/3$, $q = 0.5$ when $D = -1.5$ (a, b), $D = -1$ (c, d), and $D = -0.5$ (e, f).

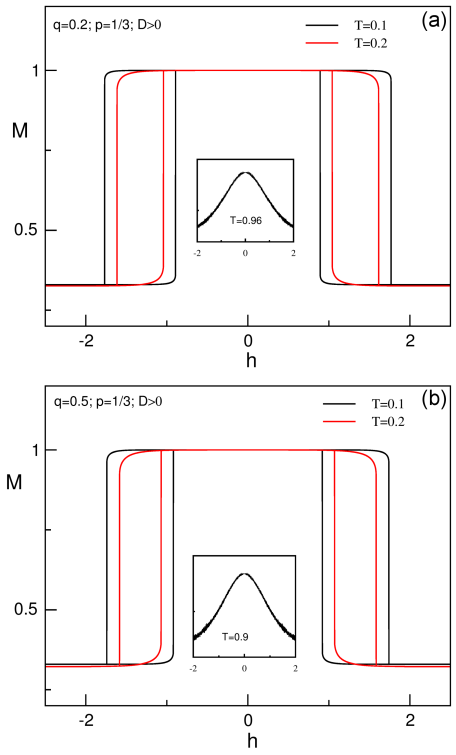

Fig. 5. Hysteresis behaviour of the system as a function of the applied field h at $T = 0.1$ or $T = 0.2$, $p = 1/3$, $D > 0$ when (a) $q = 0.2$, and (b) $q = 0.5$.

crystal field D shrink the width of loops. It should be specified that for negative values of D and fixed q, the temperature at which the hysteresis loops disappear increases with D.

In Fig. 5 mapped for $p = 1/3$, $T = 0.1$ and 0.2, with $q = 0.2$ (Fig. 5a) and $q = 0.5$ (Fig. 5b) when $D > 0$, only double hysteresis loops were obtained. At a fixed temperature T for any positive values of D, the hysteresis loops are confused, which implies that the coercive field is constant regardless of the value of D. Note that the coercive field decreases with increasing T or q. At $T = 0.1$ and for all positive values of D as q and p increase, we only observe double hysteresis loops that become narrower and disappear not only when T increases, but also when p reaches the critical value $p^* = 0.84$.

Figure 6 clearly reflects the following observations from the literature, i.e., the appearance of triple or double hysteresis loops for large negative values of D in the spin-1 BC model results from the effects of the diluted crystal field [51] or the longitudinal/transverse crystal field [52, 53] which promotes competition with other interactions existing in the system. In our case, multiple hysteresis are due to the combined action of the bimodal random crystal field and the trimodal magnetic field. These interactions force spins to flip, promoting first-order phase transitions between the two FM phases in the h range where the hysteresis loops exist.

4. Conclusions

In terms of LACVM, we studied variations of the order parameters, susceptibility and magnetic hysteresis loops under the implementations of the bimodal random crystal and trimodal random magnetic fields for the spin-1 BC model. Thermal variations of magnetic susceptibility are presented in order to confirm the existence of transition temperatures in the form of phase transitions, both first- and

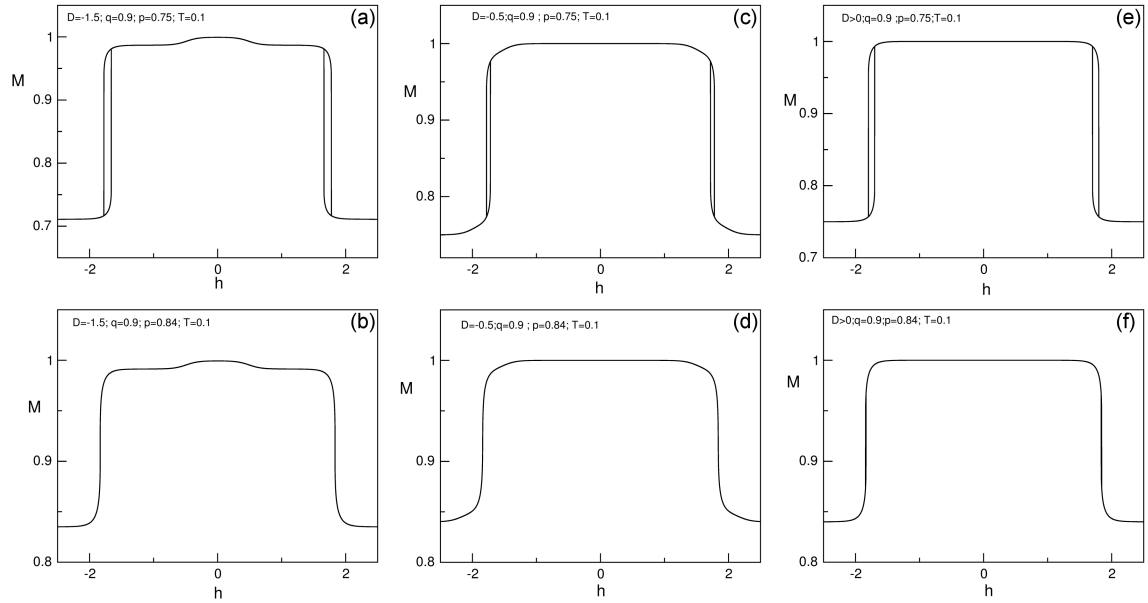

Fig. 6. Hysteresis behaviour of the system as a function of the applied field h at $T = 0.1$, $q = 0.9$, $p = 0.75$ and $p = 0.84$ when (a, b) $D = -1.5$, (c, d) $D = -0.5$, and (e, f) $D > 0$.

second-order. Reentrant behaviour observed particularly for $q = 0.2$ made it possible to account for the richness of the critical phenomena induced by the effect of these two random fields. At low temperatures, the system exhibits four and six hysteresis loops for large negative D values, and for other values only double hysteresis loops are observed. The multiple hysteresis obtained were attributed to the combined effects of two random fields. The hysteresis behaviour disappears in the system when p reaches the critical value of $p^* = 0.84$.

References

[1] P. Weiss, *J. Phys. Theor. Appl.* **6**, 661 (1907).

[2] H.A. Bethe, *Proc. Roy. Soc. London A* **150**, 552 (1935).

[3] R. Kikuchi, *Physica* **81**, 988 (1951).

[4] J.L. Morán-López, J.M. Sanchez, *Theory and Applications of the Cluster Variation and Path Probability Methods*, Plenum Press, New York 1996.

[5] M. Blume, *Phys. Rev.* **141**, 517 (1966).

[6] H.W. Capel, *Physica* **32**, 966 (1966).

[7] A. Maritan, M. Cieplak, M.R. Swift, F. Toigo, J.R. Banavar, *Phys. Rev. Lett.* **69**, 221 (1992).

[8] M. Bachmann, E. Bittner, N.G. Fytas, R. Kenna, M. Weigel, J. Zierenberg, *Eur. Phys. J. Special Topics* **226**, 789 (2017).

[9] O. Barut, A. Yigit, E. Albayrak, *J. Magn. Magn. Mater.* **513**, 167103 (2020).

[10] K. Htoutou, Y. Benhouria, A. Oubelkacem, R. Ahl laamara, L.B. Drissi, *Chin. Phys. B* **26**, 127501 (2017).

[11] A. Yigit, E. Albayrak, *Superlattices Microstruct.* **117**, 65 (2018).

[12] D.P. Belanger, in: *Spin Glasses and Random Fields*, Ed. A.P. Young, World Scientific, Singapore 1998.

[13] H. Nishimori, *Statistical Physics of Spin Glasses and Information Processing*, Oxford University Press, Oxford 2001.

[14] E. Albayrak, *J. Magn. Magn. Mater.* **324**, 1809 (2012).

[15] A. Bobák, J. Dely, *Physica A* **341**, 281 (2004).

[16] E. Albayrak, *J. Magn. Magn. Mater.* **323**, 992 (2011).

[17] Y. Yüksel, *J. Phys. Chem. Solids* **86**, 207 (2015).

[18] E. Albayrak, *Acta Phys. Pol. A* **127**, 818 (2015).

[19] E. Albayrak, *Chin. Phys. B* **22**, 077501 (2013).

[20] E. Albayrak, *Chin. J. Phys.* **56**, 622 (2018).

[21] E. Albayrak, *J. Magn. Magn. Mater.* **355**, 18 (2014).

[22] N.G. Fytas, J. Zierenberg, P.E. Theodorakis, M. Weigel, W. Janke, A. Malakis, *Phys. Rev. E* **97**, 040102(R) (2018).

[23] E. Vatansever, Z.D. Vatansever, P.E. Theodorakis, N.G. Fytas, *Phys. Rev. E* **102**, 062138 (2020).

[24] H. Magoussi, B. Boughazi, M. Kerouad, *J. Supercond. Nov. Magn.* **31**, 3817 (2018).

[25] Y.YĂźksel, H. Polat, *J. Magn. Magn. Mater.* **322**, 3907 (2010).

[26] E. Costabile, M. Amazonas, J.R. Viana, J.R. de Sousa, *Phys. Lett. A* **376**, 2922 (2012).

[27] J.R. Viana, O.D.R. Salomon, M.A. Neto, D.C. Carvalho, *Int. J. Mod. Phys. B* **32**, 1850038 (2018).

[28] C.M. Salgado, N.L. de Carvalho, P.H.Z. de Arruda, M. Godoy, A.S. de Arruda, E. Costabile, J.R. de Sousa, *Physica A* **522**, 18 (2019).

[29] O. Canko, E. Albayrak, M. Keskin, *J. Magn. Magn. Mater.* **294**, 63 (2005).

[30] E. Albayrak, *Phys. Rev. B* **65**, 134429 (2002).

[31] R.J. Creswick, H.A. Farach, J.M. Knight, C.P. Poole Jr., *Phys. Rev. B* **38**, 4712 (1988).

[32] E. Albayrak, *Physica A* **392**, 552 (2013).

[33] E. Albayrak, *Chin. J. Phys.* **54**, 978 (2016).

[34] E. Vatansever, N.G. Fytas, *Phys. Rev. E* **97**, 012122 (2018).

[35] M. Kaufman, M. Kanner, *Phys. Rev. B* **42**, 2378 (1990).

[36] P.V. Santos, F.A. da Costa, J.M. de Araújo, *J. Magn. Magn. Mater.* **451**, 737 (2018).

[37] E. Albayrak, *Chin. J. Phys* **68**, 100 (2020).

[38] R.A.A. Yessoufou, E. Albayrak, G. Seto *Chin. J. Phys.* **77**, 2713 (2022).

[39] N.G. Fytas, P.E. Theodorakis, I. Georgiou, *Eur. Phys. J. B* **85** 349 (2012).

[40] E. Albayrak, *Mod. Phys. Lett. B* **35**, 2150270 (2021).

[41] H. Magoussi, A. Zaim, M. Kerouad, *Chin. Phys. B* **22**, 116401 (2013).

[42] W.P. da Silva, P.H.Z. de Arruda, T.M. Tunes, M. Godoy, A.S. de Arruda, *J. Magn. Magn. Mater.* **422**, 367 (2017).

[43] R.E. Peierls, *Math. Proc. Cambridge Philos. Soc.* **32** 477 (1936).

[44] H.A. Kramers, G.H. Wannier, *Phys. Rev.* **60**, 252 (1941).

[45] H.A. Kramers, G.H. Wannier *Phys. Rev.* **60**, 263 (1941).

[46] M. Plischke, B. Bergersen *Equilibrium Statistical Physics*, World Scientific Publishing, Singapore 1994.

[47] D.A. Lavis, G.M. Bell, *Statistical Mechanics of Lattice Systems*, Springer, Berlin 1999.

[48] T. Morita, M. Suzuki, K. Wada, M. Kaburagi, *Prog. Theor. Phys. Suppl.* **115**, R1 (1994).

[49] A. Pelizzola, *J. Phys. A: Math. Gen.* **38**, R309 (2005).

[50] R. Kikuchi, *J. Physique* **7**, 307 (1967).

[51] U. Akinci, *Phys. Lett. A* **380**, 1352 (2016).

[52] U. Akinci, *J. Magn. Magn. Mater.* **397**, 247 (2016).

[53] S. Bouhou, I. Essaoudi, A. Ainane, M. Saber, J.J. de Miguel, M. Kerouad, *Chin. Phys. Lett.* **29**, (2012) 016101.